PHYSICAL REVIEW D **89,** 085016 (2014)

Coordinate-space singularities of massless gauge theories

Ozan Erdoğan[*]

C. N. Yang Institute for Theoretical Physics and Department of Physics and Astronomy, Stony Brook University, Stony Brook, New York 11794–3840, USA

(Received 20 December 2013; published 7 April 2014)

The structure of singularities in perturbative massless gauge theories is investigated in coordinate space. The pinch singularities in coordinate-space integrals occur at configurations of vertices which have a direct interpretation in terms of the physical scattering of particles in real space-time in the same way as for the loop momenta in the case of momentum-space singularities. In the analysis of vertex functions in coordinate space, the well-known factorization into hard, soft, and jet functions is found. By power-counting arguments, it is found that coordinate-space integrals of vertex functions have logarithmic divergences at worst.

DOI: 10.1103/PhysRevD.89.085016 PACS numbers: 11.15.Bt, 11.55.Bq

I. INTRODUCTION

The structure of singularities in perturbative gauge theories has long been a subject of study for theoretical interest and for phenomenological applications [1,2]. There is a vast literature on the subject, and most modern analyses are carried out in momentum space to calculate scattering amplitudes [3–6]. Calculations involving Wilson lines, however, are often simpler in coordinate space [7,8], and coordinate-space integrals were used for Wilson lines in the application of dual conformal invariance [9]. It is therefore natural to consider using them for amplitudes as well. The purpose of this paper is to provide a new, coordinate-space analysis of singularities in perturbation theory applicable to amplitudes for massless gauge theories.

It is well known that the momentum-space singularities of Feynman integrals in a generic quantum field theory occur at configurations of internal loop momenta that have a direct interpretation in terms of the physical scattering of on-shell particles in real space-time [10,11]. In this study, we will analyze the origin and structure of these singularities directly in coordinate space.

Massless gauge theories suffer from infrared (IR) divergences, which characterize the long-distance contributions to perturbative predictions, in addition to ultraviolet (UV) divergences, which can be removed by local counterterms. An analysis of infrared divergences in gauge theories from the point of pinch singularities of Feynman integrals over loop momenta was given by Ref. [12]. Following Ref. [13], which dealt with scalar theories, we will show that the coordinate-space singularities of massless gauge theories have the same interpretation in terms of the physical scattering of particles with conserved momenta. In contrast to momentum-space examples, however, we will see that collinear singularities are of ultraviolet nature in coordinate space and require $D < 4$ in dimensional regularization. This analysis can be applied to a variety of field-theory objects derived from Green functions, including form factors and vertex functions, Wilson lines, as well as cut diagrams for cross sections.

In a detailed analysis of vertex functions in coordinate space, we will find the factorization into hard, soft, and jet functions familiar from momentum-space analysis [14,15]. In coordinate space, the soft function is finite when the external points are kept at finite distances from each other. Therefore, ultraviolet regularization is needed only for the jets and the hard function. Adapting the power-counting technique developed for momentum space in Ref. [12], the residues of the light-cone poles of vertex functions in coordinate space will be shown to have logarithmic divergences at worst.

This paper is organized as follows: In Sec. II, a brief, general review of pinch singularities will be followed by a derivation of conditions for singularities in coordinate-space integrals together with their physical interpretations. We will also comment on the case with massive lines in Appendix A. In Sec. III, we will analyze the structure of singularities of vertex functions in coordinate space, solving the conditions for pinch singularities, first explicitly at lowest loop order and then extending the solutions to arbitrary order in perturbation theory. In Sec. IV, we will adapt the power-counting technique developed in Ref. [12] to the coordinate-space vertex functions, and show that divergences are at worst logarithmic relative to their lowest-order results at higher orders in perturbation theory. In the last section, we will discuss the approximations that can be made in the integrand to obtain the leading singularity. We will describe the "hard-collinear" and then the "soft-collinear" approximations, which will lead to factorization of jets from the hard and soft functions. Lastly, we will show that the fermionic vertex function can be approximated by a Wilson-line

[*]erdogan@insti.physics.sunysb.edu

calculation, by imposing the conditions for a pinch singularity inside the integrands.

II. ANALYSIS OF SINGULARITIES

This section treats the coordinate-space singularities of Feynman diagrams in gauge theories. The discussion is in many ways similar to the momentum-space analysis of Refs. [1,16,17]. The results of this section will be employed to identify the natural subregions of the corresponding diagrams in order to study their behavior in coordinate space.

We start our analysis with an arbitrary Feynman integral with massless lines in coordinate space. We work in $D = 4 - 2\varepsilon$ dimensions using dimensional regularization. For gauge theories, we employ Feynman gauge. The integrands in scalar and gauge theories are similar, except that in the latter case, gauge field vertices have derivatives that act on attached lines. These derivatives change the powers of denominators and produce numerator factors, which may enhance or suppress the integrals.

In coordinate space, we can represent graphical integrals schematically as

$$I(\{x_i^\mu\}) = \prod_{\text{vertices } k} \int d^D y_k \prod_{\text{lines } j} \frac{1}{[-(\sum_{kl} \eta_{jkl} X_{kl})^2 + i\epsilon]^{p_j}} \times F(x_i, y_k, D), \quad (1)$$

where the positions of internal vertices y_k^μ are integrated over all space-time for fixed external points x_i^μ. For each line, the sum over $\{X_{kl}\} = \{y_k, x_i\}$ includes all vertices, internal and external, where η_{jk} is an "incidence matrix," which takes the values $+1$ and -1 when the line j ends or begins at vertex k, respectively, and is zero otherwise. The orientation of a line is at this point arbitrary, but we will see that at singularities it is determined by the time ordering of the vertices it connects. Before the action of derivatives, the power of the denominator of line j is $p_j = 2 - \varepsilon$ for fermion lines and $p_j = 1 - \varepsilon$ for scalar and gauge field lines; however, if a derivative acts on a line, the power of its denominator is increased by 1. This expression holds for scalar and gauge theories, for which we sum over terms with different numbers of derivatives, and the functions $F(x_i, y_k, D)$ include remaining constants, group theory factors, and numerator factors, which do not affect the locations of the singularities but will matter in power counting. They are simply numerical constants for scalar theories. For theories with spin, they also carry the spin dependence, which we have suppressed here. The integrand in Eq. (1) becomes singular when a line moves to the light cone.

After combining the propagators of each line with Feynman parametrization, the integral will be of the form

$$I(\{x_i^\mu\}) = \prod_{\text{lines } j} \int_0^1 d\alpha_j \alpha_j^{p_j - 1} \delta\left(1 - \sum_j \alpha_j\right) \times \prod_{\text{vertices } k} \int d^D y_k D(\alpha_j, x_i, y_k)^{-N(\varepsilon)} \bar{F}(x_i, y_k, D), \quad (2)$$

where we have absorbed the prefactors of the parametrization into $\bar{F}(x_i, y_k, D)$, and where the common denominator is given by

$$D(\alpha_j, x_i, y_k) = \sum_j \alpha_j [-z_j^2(x_i, y_k) + i\epsilon]. \quad (3)$$

Here, α_j is the Feynman parameter of the jth line, and z_j^μ denotes the argument of its propagator, which is the coordinate difference between the vertices it connects. The overall power of the denominator is $N(\varepsilon) = \sum_j p_j(\varepsilon)$—in particular, $N(\varepsilon) = N(1 - \varepsilon)$ for a diagram with N scalar lines only. For gauge theories, for a diagram with N_g gauge field lines, N_f massless fermion lines, and V_{3g} three-vector vertices, it is given by $N(\varepsilon) = N_f(2 - \varepsilon) + N_g(1 - \varepsilon) + V_{3g}$.

The zeros of the denominator $D(\alpha_j, x_i, y_k)$ in Eq. (3) determine the positions of the poles of the integrand in Eq. (2). These poles may produce branch points of $I(\{x_i^\mu\})$, depending on whether or not they may be avoided by contour deformation in the complex (α, y) space. We recall here the summary given in Ref. [1]. In general, the singularities of a function $f(z)$ defined by a single integral,

$$f(z) = \int_C dw \frac{1}{g(z, w)}, \quad (4)$$

arise if and only if the poles $\tilde{w}(z)$ of the integrand, which are zeros of $g(z, w)$, cannot be avoided by contour deformation. This follows from a theorem proven by Hadamard [18] and happens either when one of the poles migrates to one of the end points of the contour, an *end-point singularity*, or when two or more isolated poles coalesce at a point trapping the contour between them, resulting in a *pinch singularity*.

These conditions for the existence of singularities can be generalized as necessary conditions for functions of several (external) variables that are defined by multiple integrals,

$$f(\{z_i\}) = \int_{\mathcal{H}} \prod_j dw_j \frac{1}{g(\{z_i\}, \{w_j\})}, \quad (5)$$

such as $I(\{x_i^\mu\})$ in our case. Here, the hypercontour $\mathcal{H}$ denotes the multidimensional region of integration. The set of points $S = \{\tilde{w}(\tilde{z})\}$ on which $g(\{z_i\}, \{w_j\}) = 0$ defines surfaces in the complex (z, w)-space. If $g(\{z_i\}, \{w_j\})$ factors as $g = g_1(\{z_i\}, \{w_j\}) \times \cdots \times g_r(\{z_i\}, \{w_j\})$, then there are r such singular surfaces, which may or may not intersect with each other. As in the case of an integral over

a single variable, the singularities occur when an intersection of these singular surfaces with the hypercontour $\mathcal{H}$ cannot be avoided. Summarizing the arguments presented in Ref. [1], this again happens either when a singular surface S overlaps with the boundary of $\mathcal{H}$ (*end-point singularity*) or when the hypercontour $\mathcal{H}$ is trapped between two or more singular surfaces or between two different parts of the same singular surface (*pinch singularity*). At an end point, $\mathcal{H}$ cannot be moved in the directions normal to its boundary, while at a pinch it cannot be moved away from singular regions in the direction of the normals to two (or more) singular surfaces, which are in opposite directions. In both cases, the vanishing of the gradient of $g(\{z_i\},\{w_j\})$ on S is the necessary condition:

$$\frac{\partial}{\partial w_j} g(\{z_i\},\{w_j\})\bigg|_{g=0} = 0. \tag{6}$$

In the following, we use the terminology of Ref. [17], and call the variables that parametrize directions out of the singular surface S *normal*, and those that lie in the surface *intrinsic*. The larger the volume of normal space, the less singular the integral. References [1,16,17] present pedagogical discussions of these concepts.

This reasoning enables us to derive a powerful set of necessary conditions for singularities of integrals like $I(\{x_i^\mu\})$ in Eq. (1) using the representation in Eq. (2), where a singular surface S in (α, y) space is defined by the set of points $S = \{\tilde{\alpha}, \tilde{y}\}$ on which $D(\alpha_j, x_i, y_k)$ vanishes. The singularities of Eq. (2) can come only from the end point $\alpha_j = 0$ of the α_j integral, because $D(\alpha_j, x_i, y_k)$ is linear in the α_j's. Note that $\alpha_j = 1$ is not a different end-point singularity, as it sets all α_i, $i \neq j$, to zero because of the delta function. On the other hand, there are no end-point singularities in y integrals, since they are unbounded. However, in y integrals, the contour of integration can be trapped at a pinch singular point when the two solutions of the quadratic equation $D = 0$ are equal, i.e.,

$$\frac{\partial}{\partial y_k^\mu} D(\alpha_j, x_i, y_k)\bigg|_{D(\tilde{\alpha},\tilde{y})=0} = 0. \tag{7}$$

The momentum-space analogs of these conditions are summarized as the Landau equations [10] in the literature. They were also written in coordinate space for scalar theories in Ref. [13]. In coordinate space, they are given by Eq. (7) above,

$$\alpha_j = 0 \quad \text{or} \quad z_j^2 = 0, \tag{8}$$

and

$$\sum_{\text{lines } j \text{ at vertex } k} \eta_{kj} \alpha_j z_j^\mu = 0. \tag{9}$$

The conditions in the first line come from $D = 0$, while those in the second line come from $(\partial/\partial y_k^\mu) D = 0$. The "or" in the first line is not necessarily exclusive. The condition $(\partial/\partial\alpha_j) D = 0$ for all j is equivalent to $D = 0$, since D is homogenous of degree 1 in the α_j's.

A physical interpretation of the momentum-space Landau equations was originally given by Coleman and Norton in Ref. [11]. The momentum-space analog of Eq. (9) in terms of momenta k_i^μ of lines is

$$\sum_{\text{lines } i \text{ in loop } l} \eta_{li} \alpha_i k_i^\mu = 0. \tag{10}$$

Then, with the identification of $\alpha_i k_i^\mu \equiv \Delta x_i^\mu$ with a space-time vector for each on-shell line, these relations can be thought of as describing on-shell particles propagating between the end and starting points of line i, which are separated by interval Δx_i^μ. This way, α_i is interpreted as the ratio of the time of propagation to the energy of particle i; and thus the analog of Eq. (8) states that there is no propagation for an off-shell line.

Similarly, in coordinate space, after the rescaling $\Delta\bar{x}_j^\mu = \alpha_j z_j^\mu$, Eq. (9) directly gives the same physical picture of on-shell particles propagating in space-time. The interpretation with particles propagating forward in time fixes the orientation of lines by the time ordering of vertices. Additionally, we may identify the product $\alpha_j z_j^\mu$ with a momentum vector,

$$p_j^\mu \equiv \alpha_j z_j^\mu. \tag{11}$$

Then Eq. (9) gives momentum conservation for the on-shell lines with momenta p_j^μ flowing in or out of vertex k. Moreover, with a further identification of α_j as the ratio of the energy of line j to the time component of z_j,

$$\alpha_j \equiv p_j^0 / z_j^0, \tag{12}$$

we obtain a relation between the energies and momenta of the propagating particles associated with the pinch singularities of Eq. (2):

$$p_j^\mu = E_j v_j^\mu, \quad \text{with} \quad v_j^\mu = (1, \vec{z}/z_j^0). \tag{13}$$

This is the relation between energy and momentum of free massless particles; the magnitude of their velocity is indeed $c = 1$, since $(z^0)^2 - |\vec{z}|^2 = 0$. Therefore, to each pinch singularity we can associate a physical picture in which massless particles propagate freely on the light cone between vertices, while their momenta satisfy momentum conservation at each internal vertex as well [13].

In the physical picture above, only lines on the light cone "carry" finite momenta. Lines not on the light cone—that is, lines connecting vertices at finite distances—have $\alpha_j = 0$, which by Eq. (12) sets their $p_j^\mu = 0$. In momentum

space, because the momenta of lines with $\alpha_j = 0$ do not show up in the momentum-space analog of Eq. (9), in a graphical representation, one can contract such off-shell lines to points. The resulting diagrams are called *reduced diagrams* that represent *lower-order* singularities of a Feynman diagram, while the diagram with all the lines on the mass shell (i.e. no lines with $\alpha = 0$) is said to give the *leading* singularity [1,19]. In contrast, in coordinate space, these "contracted" lines should be compared to "zero lines," with $z_j^\mu = 0$, that do not contribute to the sum in Eq. (9) either. They represent "short-distance" (UV) singularities, which occur when two connected vertices coincide at the same point, but are not *lower-order* singularities of the coordinate integral. These pinch singularities originate from the denominator of a single propagator, where the contour of integration, the real line, is pinched between two poles of the same propagator. Therefore, we will first identify such UV singularities of an arbitrary integral like Eq. (1), and then combine the rest of the denominators by Feynman parametrization to find other types of singularities from groups of lines in the remaining integrals using the Landau conditions [Eqs. (8) and (9)]. We should note that not all UV singularities give UV *divergences*. Divergences can be identified by the power-counting procedure below.

As an example of the application of Eq. (7) to coordinate-space integrals, we shall now find the configurations of lines for pinches in the integration over the position of a single three-point vertex at a point y^μ. For simplicity, let us consider the following integral in a scalar theory:

$$I(x_1, x_2, x_3) = \int d^D y \prod_{i=1}^{3} \frac{1}{[-(x_i - y)^2 + i\epsilon]^{1-\varepsilon}}. \quad (14)$$

Apart from the UV singularities when $y^\mu = x_i^\mu$ for $i = 1, 2$ or 3, the conditions for a pinch between different lines in the y^μ integral are given by Eqs. (8) and (9) after Feynman parametrization,

$$\alpha_1 z_1^\mu + \alpha_2 z_2^\mu + \alpha_3 z_3^\mu = 0, \quad (15)$$

with $z_i^\mu \equiv x_i^\mu - y^\mu$. For a pinch singularity, these vectors are either lightlike, $z_i^2 = 0$, or have $\alpha_i = 0$. Equation (15) cannot be satisfied if all three vectors have positive entries. Thus, at least one external point must have $x_i^+ < y^+$ and one must have $x_j^+ > y^+$, so that there is at least one incoming and one outgoing line. These considerations naturally provide a time ordering for vertices and a direction for lines at any singularity. Assuming all $\alpha_i \neq 0$ and that all lines are on the light cone, $z_i^2 = 0$ and Eq. (15) imply that $z_j \cdot z_k = 0$ as well. That is, all of these lines are parallel. If any one of the lines is off the light cone with $\alpha_i = 0$, then the other two are on the light cone and again parallel to each other by Eq. (15). These pinch singularities can be interpreted as a merging or splitting of three particles, which occurs at point y^μ, with the ratios of their momenta given by the ratios of the α_i's. Note that these results hold for the three-point vertices of a gauge theory as well, and can be generalized to n-point vertices. The coordinate-space singularities of Green functions represent physical particle scattering and thus can be related naturally to physical scattering amplitudes.

III. COORDINATE-SPACE SINGULARITIES AT A VERTEX

We will now study how coordinate-space singularities in a vertex function in a massless gauge theory emerge from pinches in Feynman integrals in perturbation theory. For simplicity, the first example that we consider will be the correlation of two scalar fields with a color-singlet gauge current. We also discuss the correlation of fermions with the same kind of current. The results of Sec. II will be applied to identify the configurations that can lead to singularities of such vertex functions in coordinate space.

The scalar vertex function of interest is obtained from the vacuum expectation value of the time-ordered product of two charged scalar fields with an incoming color-singlet current,

$$\Gamma_S^\nu(x_1, x_2) = \langle 0|T(\Phi(x_2) J^\nu(0) \Phi^*(x_1))|0\rangle. \quad (16)$$

Here, we have shifted the position of the current to the origin using the translation invariance of the vacuum state. $\Gamma_S^\nu(x_1, x_2)$ transforms as a vector under Lorentz transformations. Its functional form is well known and is determined by the Abelian Ward identity,

$$-i(\partial_1 + \partial_2)_\nu \Gamma_S^\nu(x_1, x_2) = [\delta^D(x_2) - \delta^D(x_1)] G_2((x_2 - x_1)^2), \quad (17)$$

where G_2 is the scalar two-point function, which is only a function of the invariant distance between the external points. A general solution to this inhomogenous partial differential equation can be given by a particular solution that satisfies Eq. (17) plus the general solution to the homogenous equation,

$$(\partial_1 + \partial_2)_\mu \Gamma_{S,(H)}^\mu(x_1, x_2) = 0. \quad (18)$$

A particular solution to the Abelian Ward identity, which has the structure of the lowest-order result, is given by

$$\Gamma_{S,(I)}^\nu(x_1, x_2, \mu) = \left(\frac{x_2^\nu}{(-x_2^2 + i\epsilon)^{1-\varepsilon}} - \frac{x_1^\nu}{(-x_1^2 + i\epsilon)^{1-\varepsilon}} \right) \times \frac{\Sigma_S(\mu^2 (x_2 - x_1)^2)}{x_1^2 x_2^2}, \quad (19)$$

where the form factor $\Sigma_S(\mu^2(x_2 - x_1)^2)$ is a dimensionless function, with μ^2 the renormalization scale, and it is related to the renormalized scalar two-point function by

$$iG_2(x^2,\mu^2)=\frac{\Sigma_S(\mu^2x^2)}{(-x^2+i\epsilon)^{1-\varepsilon}}. \tag{20}$$

Note that at zeroth order, one obtains $\Sigma^{(0)}(x_1,x_2)=1$ from both equations above.

The general solution to the homogenous equation can be found easily in momentum space, since one then has an algebraic equation,

$$(p_1^\mu-p_2^\mu)\tilde{\Gamma}^\mu_{S,(H)}(p_1,p_2)=0, \tag{21}$$

whose solution involves polynomials of momenta times one independent function.[1] Here, momentum p_1 flows into the vertex and p_2 out. The general solution in momentum representation is given by

$$\tilde{\Gamma}^\mu_{S,(H)}(p_1,p_2)=[(p_2^2-p_1\cdot p_2)p_1^\mu + (p_1^2-p_1\cdot p_2)p_2^\mu]\tilde{f}_H(p_1,p_2). \tag{22}$$

After inverse Fourier transform with $p_1^\mu\to i\partial_1^\mu$ and $p_2^\mu\to -i\partial_2^\mu$, the part of the vertex that vanishes in the Abelian Ward identity [Eq. (17)] is of the form

$$\Gamma^\mu_{S,(H)}(x_1,x_2)=-i(\partial_1-\partial_2)_\nu[\partial_1^\mu\partial_2^\nu-\partial_1^\nu\partial_2^\mu]f_H(x_1,x_2), \tag{23}$$

where f_H is a function of mass dimension 2. In conventional terms, the inhomogenous solution gives the "longitudinal" part of the vertex, while the homogenous solution is the "transverse" part. Note that any f_H that is a function of only $(x_1\pm x_2)^2$ vanishes under the derivatives in Eq. (23). Thus, f_H must depend on x_i^2 separately to contribute to the scalar vertex. This will allow light-cone singularities to factorize from the rest of the vertex.

The fermionic counterpart of Eq. (16) is

$$(\Gamma_F)^\nu_{ba}(x_1,x_2)=\langle 0|T(\psi_b(x_2)J^\nu(0)\bar{\psi}_a(x_1))|0\rangle, \tag{24}$$

whose tensor and Dirac structure is determined by the invariance under the global symmetries of the theory, while its functional form is similarly constrained by the Ward identity for fermion fields. Chiral invariance for a massless theory requires this vertex to have an odd number of gamma matrices. Skipping the details given for scalars above, a particular solution for the "longitudinal" part of the fermionic vertex function is given by

$$(\Gamma_{F,(I)})^\nu_{ba}(x_1,x_2,\mu)=\frac{(\not{x}_2\gamma^\nu\not{x}_1)_{ba}}{(-x_2^2+i\epsilon)^{2-\varepsilon}(-x_1^2+i\epsilon)^{2-\varepsilon}}\times\Sigma_F(\mu^2(x_2-x_1)^2), \tag{25}$$

where $\Sigma_F(x^2)$ is related to the renormalized fermion two-point function $S_F(x^2)$ by

$$iS_F(x^2,\mu^2)=\not{x}\frac{\Sigma_F(\mu^2x^2)}{(-x^2+i\epsilon)^{2-\varepsilon}}. \tag{26}$$

The "transverse" part of the fermionic vertex function that vanishes in the Abelian Ward identity can be written in the form

$$\begin{aligned}\Gamma^\mu_{F,(H)}(x_1,x_2)=&\gamma^\mu[(\Box_1+2\partial_1\cdot\partial_2+\Box_2)f_1(x_1,x_2)+(\Box_1-\Box_2)f_2(x_1,x_2)]-(\partial_1+\partial_2)(\partial_1+\partial_2)^\mu f_1(x_1,x_2)\\&-(\partial_1+\partial_2)(\partial_1-\partial_2)^\mu f_2(x_1,x_2)+(\partial_1-\partial_2)(\partial_1+\partial_2)_\nu(\partial_2^\nu\partial_1^\mu-\partial_1^\nu\partial_2^\mu)f_3(x_1,x_2)\\&+\gamma_5\epsilon^{\mu\nu\rho\sigma}\gamma_\nu(\partial_1-\partial_2)_\rho(\partial_1+\partial_2)_\sigma f_4(x_1,x_2).\end{aligned} \tag{27}$$

Here, all form factors $f_i(x_1,x_2)$ have mass dimension 4 except $f_3(x_1,x_2)$, which has dimension 2. The tensor decomposition of this vertex and the list of form factors in momentum space can be found in Ref. [20]. Again, these form factors can have arbitrary dependence on x_i^2, which allows factorization of light-cone singularities.

We are interested in singularities that are related to scattering processes; thus, the limit $x_1\to x_2$ will not be considered in the discussion below, as it gives effectively a two-point function. We also assume here that x_1^μ and x_2^μ are fixed, nonzero vectors that are not lightlike separated $(x_1\cdot x_2\neq 0)$. Given these external data, the only power singularities of the coordinate-space vertex functions will be in x_i^2, which correspond to single-particle poles of the external propagators in momentum space. Furthermore, both $\Sigma_S(x_1,x_2)$ in Eq. (19) and $\Sigma_F(x_1,x_2)$ in Eq. (25) remain finite when $x_i^2=0$ with $x_1\cdot x_2\neq 0$. Thus, the leading divergence of the scalar vertex can come from $f_H(x_1,x_2)$ in Eq. (23), while the leading divergence of the fermionic vertex comes along again from the "transverse" part of the vertex.

Let us now illustrate how the light-cone singularities of the vertex functions given above emerge at one loop in perturbation theory. The integrand of the one-loop diagram in Fig. 1, the first nontrivial contribution to the scalar vertex function, is of the form

[1]Starting from $(p_1-p_2)_\mu(Ap_1^\mu+Bp_2^\mu)=0$, the homogenous equation is solved for $\frac{A}{B}=\frac{p_2^2-p_1\cdot p_2}{p_1^2-p_1\cdot p_2}$. The Ward identity reduces the number of independent functions by 1.

$$\Gamma_S^{(1)\mu}(x_1,x_2) = C_S^{(1)} \int d^D y_1 d^D y_2 g^{\alpha\beta} \frac{1}{[-(y_2-y_1)^2+i\epsilon]^{1-\varepsilon}} \left(\frac{1}{[-(x_2-y_2)^2+i\epsilon]^{1-\varepsilon}} \overleftrightarrow{\partial}_{y_2^\alpha} \right.$$
$$\left. \left[\frac{1}{[-(y_2-z)^2+i\epsilon]^{1-\varepsilon}} \overleftrightarrow{\partial}_{z^\mu} \frac{1}{[-(z-y_1)^2+i\epsilon]^{1-\varepsilon}} \right]_{z=0} \overleftrightarrow{\partial}_{y_1^\beta} \frac{1}{[-(y_1-x_1)^2+i\epsilon]^{1-\varepsilon}} \right), \tag{28}$$

with $C_S^{(1)}$ a numerical constant. Compare this expression to that of the one-loop diagram for the fermionic vertex function,

$$\Gamma_F^{(1)\mu}(x_1,x_2) = C_F^{(1)} \int d^D y_1 d^D y_2 \frac{1}{[-(y_2-y_1)^2+i\epsilon]^{1-\varepsilon}} \left(\partial_{x_2} \frac{1}{[-(x_2-y_2)^2+i\epsilon]^{1-\varepsilon}} \right) \gamma^\alpha$$
$$\times \left(\partial_{y_2} \frac{1}{[-y_2^2+i\epsilon]^{1-\varepsilon}} \right) \gamma^\mu \left(\partial_{y_1} \frac{1}{[-y_1^2+i\epsilon]^{1-\varepsilon}} \right) \gamma_\alpha \left(\partial_{x_1} \frac{1}{[-(y_1-x_1)^2+i\epsilon]^{1-\varepsilon}} \right). \tag{29}$$

Clearly, both have the same pole structure—more precisely, the positions of the poles are the same, although term by term their degrees may or may not be different. Using Feynman parametrization either before or after the action of the derivatives on the lines, both integrals can be put into the form of Eq. (2) with the same common denominator, but, of course, with different numerator factors and different powers of the resulting denominator in the integrands.

The pinch singularities of Eqs. (28) and (29) can originate from the two poles of a single denominator or from poles from different denominators. For the latter case, we will combine the denominators by Feynman parametrization and use Eq. (7), the coordinate-space analog of Landau equations. In general, at a pinch singularity, one encounters combinations of these two cases simultaneously. After Feynman parametrization, the common denominator for either diagram is given by

$$D^{(1)}(x_1,x_2,y_1,y_2;\{\alpha\}) = -\alpha_1(y_1-x_1)^2 - \alpha_2 y_1^2 - \alpha_3 y_2^2 - \alpha_4(x_2-y_2)^2 - \alpha_5(y_2-y_1)^2 + i\epsilon. \tag{30}$$

Using Eq. (7), we get the Landau conditions for pinches in the integration over the positions of internal vertices y_1 and y_2,

$$\alpha_1(y_1-x_1)^\mu + \alpha_2 y_1^\mu - \alpha_5(y_2-y_1)^\mu = 0, \tag{31}$$

$$-\alpha_4(x_2-y_2)^\mu + \alpha_3 y_2^\mu + \alpha_5(y_2-y_1)^\mu = 0, \tag{32}$$

when $D^{(1)}$ vanishes at a singularity.

We shall list the singularities of Eqs. (28) or (29) starting with pinches without any zero lines. Equations (31) and (32) make up an underdetermined system of two vector equations, since the α_j's also are unknowns. We will not list all solutions to these equations, but only those that give the leading power singularities of the vertex functions, which are physically relevant. By leading power singularities of the vertex functions, we mean the terms in

$$\hat{\Gamma}^\mu_{S,F}(x_1,x_2) = x_1^2 x_2^2 \Gamma^\mu_{S,F}(x_1,x_2) \tag{33}$$

that do not vanish when $x_1^2 = x_2^2 = 0$. The simplest solution is when only $\alpha_5 = 0$ while others are nonzero, where one gets

$$y_1^\mu = \frac{\alpha_1}{\alpha_1+\alpha_2} x_1^\mu, \tag{34}$$

$$y_2^\mu = \frac{\alpha_4}{\alpha_3+\alpha_4} x_2^\mu, \tag{35}$$

such that y_1^μ becomes "parallel" to x_1^μ while y_2^μ is parallel to x_2^μ. The necessary condition for a singularity, $D^{(1)} = 0$, is then satisfied only if $x_1^2 = x_2^2 = 0$. This solution can be interpreted as a "soft" gauge particle, say a gluon, propagating over a finite (invariant) distance between y_1 and y_2, such that the directions of the external particles have not changed after the emission or absorbtion of the gluon. In momentum space, lines with negligible momenta are called soft, while in coordinate space, soft lines are those which connect two points at a finite (invariant) distance. In this case, the scalar/fermion lines are on the light cone for a pinch.

If α_5 were not equal to zero, the general solution to Eqs. (31) and (32) is such that y_1^μ, and similarly y_2^μ, are given

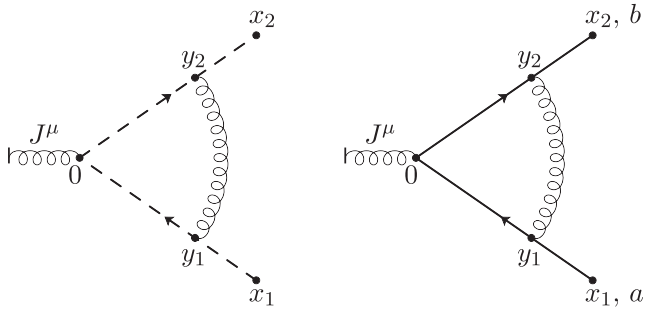

FIG. 1. One-loop diagrams for the vertex functions in Eqs. (16) and (24).

as linear combinations of x_1^μ and x_2^μ. Assuming no other α_j vanishes either, $D^{(1)}=0$ requires then not only $x_i^2=0$ but also $x_1^\mu \cdot x_2^\mu = 0$. These solutions, however, imply that x_1 and x_2 are lightlike separated. Likewise, when only $\alpha_2=0$ or $\alpha_3=0$, the condition $D^{(1)}=0$ is only satisfied with x_1 and x_2 lightlike separated. On the other hand, if $\alpha_1=0$, the solution to Eq. (31) is such that $y_1^\mu \propto y_2^\mu$, and by Eq. (32), both y_1 and y_2 are then parallel to x_2, with $D^{(1)}=0$ being satisfied for $x_2^2=0$. However, now the external line $(x_1-y_1)^2$ cannot be on the light cone, so that this solution does not correspond to a leading power singularity of the vertex. Similarly, when $\alpha_4=0$, y_1 and y_2 will be parallel to x_1, and $D^{(1)}=0$ is satisfied for $x_1^2=0$, so that the external line $(x_2-y_2)^2$ cannot be on the light cone either. The solutions with two or more α_j's vanishing are either ruled out because of the reasons given above or because they are equivalent to singularities from zero lines with $z_j^\mu(y_i)=0$, which we now consider below.

Let us first consider the UV-type singularity of the internal line connecting the vertex at y_1 to the origin, $y_1^\mu=0$, and look at the conditions for pinches in the remaining integral over y_2^μ. Equation (32) is now satisfied for

$$y_2^\mu = \frac{\alpha_4}{\alpha_3+\alpha_4+\alpha_5} x_2^\mu. \tag{36}$$

Similarly, when $y_2^\mu=0$, Eq. (32) gives

$$y_1^\mu = \frac{\alpha_1}{\alpha_1+\alpha_2+\alpha_5} x_1^\mu. \tag{37}$$

These solutions satisfy the condition $D^{(1)}=0$ if $x_2^2=0$ and $x_1^2=0$, separately. According to the physical interpretation of pinch singularities given in the previous section, these solutions give "collinear" gauge particles that propagate on the light cone parallel to one of the external scalars/fermions. We will refer to such lightlike lines with finite energies and momenta in the physical interpretation as "jet lines."

Next, consider the case when both internal vertices move to the origin, $y_1^\mu=y_2^\mu=0$, which makes three lines become zero lines simultaneously. Again, the vanishing of $D^{(1)}$ for a singularity requires $x_1^2=x_2^2=0$ with all lines on the light cone; otherwise $\alpha_1=\alpha_4=0$. This solution represents an ultraviolet (short-distance) divergence, and we call it a "hard" solution by analogy to hard scattering.

Among the remaining cases with zero vectors, first consider $y_2^\mu=x_2^\mu$ and $y_1^\mu=x_1^\mu$. The solution to Eq. (31) for the former, and to Eq. (32) for the latter, is such that y_1^μ, and similarly y_2^μ, is given as a linear combination of x_1^μ and x_2^μ, so that $D^{(1)}=0$ is not satisfied for these (unless $\alpha_5=0$) because $x_1^\mu \cdot x_2^\mu \neq 0$. For $y_1^\mu=y_2^\mu=y^\mu$, both of the external lines cannot be on the light cone simultaneously. Among the cases when two propagators have zero arguments at the same time, $y_1^\mu=x_1^\mu$ together with $y_2^\mu=0$, as well as $y_1^\mu=0$ together with $y_2^\mu=x_2^\mu$, are limiting cases of collinear solutions in Eqs. (37) and (36), respectively, while any other combination is ruled out because they require $x_i^2=0$ and $x_1\cdot x_2=0$. The only possible solution with three zero lines is the hard solution we found, and there cannot be any other with more zero lines, because $x_1^\mu \neq x_2^\mu \neq 0$. We have finished the list of solutions to Landau conditions for the leading power singularities of the vertex functions at one loop.

From the solutions to Landau conditions at one loop, one can draw the conclusion that the divergences of the vertex functions in coordinate space come from configurations where, whether the gluons are soft or collinear, the external particles move along *rigid, classical* trajectories along the directions of external points that are located on the light cone. For the singular configurations at higher orders, we will not need to solve the Landau equations explicitly. Instead, we will make use of the physical interpretation of the necessary conditions for a pinch singularity given in the previous section, and confirmed above for the one-loop case.

In the case of the pinch singularities of the vertex function, to identify an arbitrary pinch surface, we can use the necessary condition in Eq. (9) that the lightlike lines of the corresponding diagram must describe a physical process, where the two external lines start from the same point, say the origin, moving in different directions, toward x_1^μ and x_2^μ. For the sake of the argument, suppose the external particles are fermions. Any gauge field lines that connect them by vertices at finite distances have to be soft, because they cannot be parallel to both. They may still have a hard interaction at the origin reflecting a short-distance singularity. The integrals over the positions of the fermion-gluon vertices will be pinched either when the gluon and the fermion lines get mutually collinear, or when the two collinear fermions are connected by the emission of a soft gluon as described in the example given at the end of Sec. II. Likewise, the integrations over the positions of vertices to which these collinear gluons are connected will be pinched if the other lines connected to these vertices also become parallel to them, such that all collinear lines make up a "jet" moving in the direction of the external fermions. The Landau conditions allow these collinear gluons to emit soft gluon lines that can connect to the other jet as well. Therefore, the two jets can have hard interactions at very short distances, and they can only interact by the exchange of soft partons at long distances at later times. Eventually, the fermion lines end at the external points x_i^μ, which have to be on the light cone, $x_i^2=0$, in order for $D^{(n)}=0$ to be satisfied.

To sum up, the pinch singularities of the integrals for vertex functions in coordinate space come from configurations where the (time-ordered) vertices, at which either soft or collinear gluons are emitted or absorbed, are aligned along *straight* lines going through the "origin" and the external points. These two lines also determine the classical

trajectories of the external particles in the Coleman-Norton interpretation. The behavior of the integrals for arbitrary diagrams at higher orders near the corresponding pinch surfaces will be covered by general power-counting arguments in the next section.

IV. POWER COUNTING

In this section, we will apply a power-counting technique similar to the one developed for momentum-space integrals in Ref. [12] to study the behavior of the divergences of vertex functions in coordinate space. We have studied in the previous section the pinch singularities in the integrals when the external points are on the light cone. As the external propagators are not truncated, even the zeroth-order results are very singular in coordinate space when the external points are on the light cone; for instance, the fermionic vertex diverges as $1/(x_1^2x_2^2)^2$. Therefore, we will now only consider the external points set on the light cone and look for the degree of divergence of vertex functions with respect to their lowest-order results. In a sense, we are looking for any possible divergences in the residues of the light-cone poles, by analogy to the residues of single-particle poles in external momenta of Green functions in momentum space for S-matrix elements. We will show at the end of this section by power-counting arguments that vertex functions in coordinate space have at worst logarithmic divergences with respect to their lowest-order results at higher orders in perturbation theory.

Since $x^2 = 0$ does not imply $x^\mu = 0$ in Minkowski space, naïve dimensional counting does not neccessarily bound the true behavior of the integrals. As we already mentioned in Sec. II, the divergences of the integrals are related to both the volume of the space of normal variables and the singularities of the integrand. Therefore, we will do the power counting by combining the size of the volume element of normal variables with that of the integrand, which depends on both normal and intrinsic variables. In order to estimate the size of the integrand, we will first approximate the integrals near the pinch surfaces by keeping in each factor (numerator or denominator) only the terms of lowest order in normal coordinates, as their scale goes to zero. Then the resultant integrand is a homogenous function of normal variables, and the powers of the normal variables in the homogenous integrals combined with the *normal volume element* will give us the bounds on the original integrals.

Suppose $z_1, \ldots, z_n$ and $w_1, \ldots, w_m$ denote the normal and intrinsic variables for a pinch surface S of an integral I. The z_i's vanish on S with a scale λ, while the w_j's remain finite (as $\lambda \to 0$) on S. For our discussion for vertex functions, we can choose a single scale λ for properly chosen normal coordinates in our integrals to do the power counting, although we should stress that this does not need to be the case in general. The scale λ bounds the size of each normal variable and measures the "distance" of the hypercontour $\mathcal{H}$ from the pinch surface S. The homogenous integral $\bar{I}$ near the pinch surface S will have the form[2]

$$\bar{I} \sim \int d\lambda^2 \int_{\mathcal{H}} \left(\prod_{i=1}^{n} dz_i\right) \delta\left(\lambda^2 - \sum_i |z_i|^2\right) \times \int \left(\prod_{j=1}^{m} dw_j\right) \bar{f}(z_i, w_j), \tag{38}$$

where the homogenous integrand $\bar{f}(z_i, w_j)$ is obtained by keeping only terms of lowest order in λ in each factor of the original integrand such that

$$f(z_i, w_j) = \lambda^{-d_H} \bar{f}(z_i', w_j)(1 + \mathcal{O}(\lambda)) \tag{39}$$

for each normal variable $z_i = \lambda z_i'$, with d_H the degree of homogeneity of $\bar{f}(z_i, w_j)$. More specifically, as we will do the analysis for integrals of the form of Eq. (1), d_H equals the sum of the lowest powers of λ in the denominator factors minus that in the numerator factors in $f(z_i, w_j)$. The idea is then to scale out λ from each factor in the homogenous integral, to count the overall power, and find the behavior of the integral as $\lambda \to 0$,

$$\bar{I} \sim \int d\lambda \lambda^{\gamma-1} \int_{\mathcal{H}} \prod_{i=1}^{n} dz_i' \delta\left(1 - \sum_i |z_i'|^2\right) \int \prod_{j=1}^{m} dw_j \bar{f}(z_i', w_j), \tag{40}$$

where the overall degree of divergence γ is given by

$$\gamma = n - d_H. \tag{41}$$

By overall degree of divergence, we mean the power of scale parameter λ in the overall integral when all normal variables have the same scale. For $\gamma = 0$, the divergences are logarithmic, while for $\gamma < 0$ there will be power divergences.

If some set of normal coordinates vanished faster than others on S, say as λ^2, that would only increase the power of λ in the volume element of the normal space, giving a nonleading contribution, unless there are new pinches in the homogenous integral after dropping terms that are higher order in the normal variables. These pinches, which could occur between poles that were separated by nonleading terms before they were dropped, could enhance the integrals in principle. However, we will argue that, for our choice of variables, only pinches of the hard/jet/soft type occur in the homogenous integrals. Notice also that, if every normal variable in a subregion vanishes faster than

[2]This form, with a delta function having the sum of the squares of the absolute values of the normal variables in its argument, corresponds to bounding the normal space with an n-dimensional sphere with radius λ.

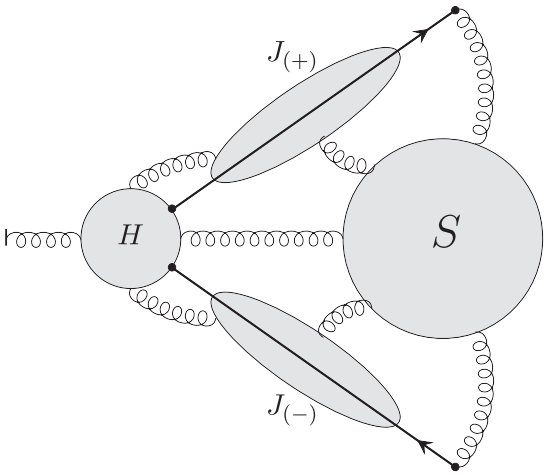

FIG. 2. Illustration of the soft (S), hard (H), and jet ($J_{(\pm)}$) regions.

those of other regions, the power counting will still be the same for each subregion. Before two lines can produce a pinch singularity, they must approach the hypercontour to the same scale. Therefore, one can choose a single scale for all normal variables for the power counting for a particular vertex function near a pinch surface. We shall now apply this power-counting technique for the fermionic vertex given by Eq. (24), which we will refer to as the vertex function in the following. As we shall see, power counting for the scalar vertex is essentially equivalent.

As we are dealing with lightlike lines, we will use light-cone coordinates, because the Landau equations for light-cone singularities can be solved more simply in these coordinates. By a combination of rotations and boosts, one can put one of the external points at $x_2^\mu = X_2\delta^{\mu+}$ and the other one at $x_1^\mu = X_1\delta^{\mu-}$, giving $x_1^2 = x_2^2 = 0$ with $x_1 \cdot x_2 \neq 0$. This will set our coordinate system.

For a particular pinch surface S, i.e. a particular solution to the Landau equations, one has to identify the intrinsic and normal variables that parametrize the surface and its normal space, respectively. For instance, let us take the solution with a soft gluon at one loop from Sec. III. There, y_2^+ and y_1^- are the intrinsic variables that remain finite, while y_2^-, y_1^+, $y_{2,\perp}^2$, and $y_{1,\perp}^2$ are the normal variables that vanish on the pinch surface. Such lines connecting vertices at finite distances are part of the soft function. On the other hand, for the hard solution at one loop, all components of y_1^μ and y_2^μ are vanishing, and one has only normal variables for this solution. We will refer to the set of lines connecting a set of vertices all of whose coordinates vanish as the "hard" function. Lastly, in the one-loop example, there were collinear lines. At one loop, for a line in the plus direction, y_2^+ is the intrinsic variable, while the rest of the components are normal variables. The set of collinear gluons, together with the external lines to which they are parallel, define the jet function and its direction. Note that the limits of integration of y_2^+ here go from zero up to X_2 on this pinch surface. For $y_2^+ > X_2$, the Landau equations cannot be solved. Indeed, $y_2^+ > X_2$ does not correspond to a physical process where all lines move forward in time. In general, in a jet, the limits of integration over the intrinsic variables for a given pinch surface are not unbounded, but are set according to the time ordering of vertices along the jet direction.

In homogenous integrals, the denominators of the jet lines will be linear, and those of the hard lines will be quadratic in normal variables, while the soft lines are of zeroth order. The lines connecting the hard function with the jets are linear in normal variables, and we thus count them as part of the jets. Any line connecting the jets or the hard part to the soft function is zeroth order in normal variables, and hence they are counted in the soft function.

The only approximation in writing the homogenous integrand is dropping terms that are of higher order in the normal variables. In fact, such terms occur only in lines connecting two different subdiagrams, namely, in lines connecting the jets to the hard and soft function or those connecting the hard and soft functions. In order for our power-counting arguments to be valid, there must not be new pinches introduced in the homogenous integrals because of this approximation. In other words, the Landau conditions for the homogenous integral to be pinched must have the same solutions as those of the original integral (up to trivial shifts or rescalings in some of the variables). We mean by "the same solutions" that the pinch singularities of both have the same physical picture. Note that soft lines are never pinched in coordinate space, and thus we only need to consider the pinches of the lines connecting a jet to the hard part in the original and homogenous integrals. To this end, one may consider, for instance, the following integral over two jet lines, which is a part of a jet function:

$$I = \int d^4y \frac{1}{-(x-y)^2 + i\epsilon} \frac{1}{-(y-z)^2 + i\epsilon}, \qquad (42)$$

where x^μ, y^μ are jet vertices and z^μ is a hard vertex.[3] The Landau conditions for a pinch from these two lines after Feynman parametrization are given by

$$-\alpha_1(x-y)^\mu + \alpha_2(y-z)^\mu = 0, \qquad (43)$$

with $(x-y)^2 = (y-z)^2 = 0$. The only solution to these conditions is that all three vertices are aligned along the jet direction, say the plus direction, and are parallel to each other. The vertex z^μ is allowed to be hard by these conditions, i.e. z^+ can also vanish in Eq. (43) at the same rate as the other components. If one approximates the

[3]Here, we have omitted the derivatives at each vertex in order to write a simple integrand to illustrate the idea.

integral in Eq. (42) by a homogenous integrand with $(y-z)^2 \sim y^2 - 2y^+z^-$, the condition for a pinch in the y^- integral is then the same as the condition [Eq. (43)] for the original integral with $z^+ = 0$. The integrals over the transverse components of y^μ can only be pinched at $y_\perp^2 = x_\perp^2 = 0$. These pinch singularities are present in both the original and homogenous integrals. They show up as end-point singularities after the change of variables with y^1, $y^2 \to y_\perp^2$, ϕ, which can always be carried out. In general, the pinches of the homogenous integral correspond to pinches of the original integral with some of the variables moved to their end points.

This approximation can fail if z^+ becomes comparable to y^+ and x^+, or if y^+ diminishes like z^+, which are actually different solutions to the Landau conditions corresponding to different pinch surfaces. Nevertheless, we will see that the result of power counting will not differ in either case, whether the vertex z^μ is taken as part of the jet, or included in the hard part. In our analysis, we identify the normal variables of a pinch surface, group each vertex in a certain subdiagram depending on the size of the components of its position, and do the power counting for the divergence on that particular pinch surface. Generally speaking, the approximations in the homogenous integrals can change if two different regions overlap when some vertices escape to a different subdiagram. However, we will show that the changes in the powers of the factors of two subdiagrams due to removal of a vertex from one subdiagram and its inclusion in the other subdiagram cancel each other, leading to the same conclusion for the overall degree of divergence.

A. Power counting for a single jet

Before we do the power counting for the full vertex function in coordinate space, we begin with the power counting for a single jet, with the topology of a self-energy diagram, as depicted in Fig. 2. Let us take a "dressed" ultrarelativistic fermion moving in the plus direction, so that the plus coordinates of all vertices inside the jet are the intrinsic variables, while their minus coordinates and squares of transverse positions are the normal variables. With these choices, all normal variables appear linearly in jet-line denominators. The condition that the vertices have to be on the light cone for pinches leaves us with three variables for each vertex. The azimuthal symmetry around the jet axis allows us to choose the square of the transverse components as one normal variable. We will compute the contributions to the overall degree of divergence of the jet, γ_J, from the normal volume element, the denominators, and the numerators of the jet function as defined in Eq. (41) for a generic singular integral.

For every integration over the positions of the three- and four-point vertices inside the jet, one needs to add $+2$ to γ_J; that is, $+1$ for each normal variable (transverse square and minus component). In $D = 4 - 2\varepsilon$ dimensions, however, the power for transverse square components is $+(1-\varepsilon)$. In the homogenous jet function, the denominator of each gauge field line contributes a term $-(1-\varepsilon)$, while that of each fermion line contributes $-(2-\varepsilon)$ to γ_J, since the massless fermion propagator in coordinate space is given, as in Eq. (29), by

$$S_F(x) = \partial\Delta_F(x^2) = \frac{\Gamma(2-\varepsilon)}{2\pi^{2-\varepsilon}} \frac{\not{x}}{(-x^2+i\epsilon)^{2-\varepsilon}}. \quad (44)$$

We are interested in the degree of divergence with respect to the lowest-order result, so we will multiply the diagrams of Fig. 3 by $[\not{x}/(-x^2+i\epsilon)^{2-\varepsilon}]^{-1}$. Equivalently, we add a term $+(2-\varepsilon)$ to γ_J to cancel the light-cone divergence of the lowest-order diagram, which is simply the fermion propagator.

Now we consider the numerator suppressions. In order to get the leading divergences, in the numerators we will keep only the terms of lowest order in normal coordinates, which therefore give the least suppression. To begin, we note that there is a factor contributing to the numerator from each fermion-gluon vertex at a point y_n^μ of the form

$$(\not{y}_{n+1}-\not{y}_n)\gamma^\mu(\not{y}_n-\not{y}_{n-1}) = 2(y_{n+1}-y_n)^\mu(\not{y}_n-\not{y}_{n-1}) - \gamma^\mu(\not{y}_{n+1}-\not{y}_n)(\not{y}_n-\not{y}_{n-1}). \quad (45)$$

Here, the first term is unsuppressed as it is, although the vector with the index μ must form an invariant with some other vector. At the same time, terms proportional to γ^μ in Eq. (45) either vanish by $(\gamma^\mp)^2 = 0$ or vanish at least as the transverse coordinates of one of the vertices, which are at the order of $\lambda^{1/2}$. In the case of scalar, instead of gauge field lines, with Yukawa couplings to fermions, for each two-fermion-scalar vertex there would be a factor of $(\not{y}_{n+1}-\not{y}_n)(\not{y}_n-\not{y}_{n-1})$ in the numerator, giving the same power-counting suppression of at least $\lambda^{1/2}$.

In addition to numerator factors from fermion lines, there are factors from three-gluon vertex functions. A vertex at z_m^μ combines with gluon propagators to give terms that (dropping overall factors) can be written as

$$v_{3g}(z_m,\{y_i\}) = \epsilon_{ijk}g^{\mu_i\mu_j}\Delta(z_m-y_i)\Delta(z_m-y_j) \times \partial_{z_m}^{\mu_k}\Delta(z_m-y_k), \quad (46)$$

where the y_i's are the positions of the other ends of the lines. Acting on the gluon lines, the derivatives bring vectors from their coordinate arguments to the numerator, while increasing the power of a denominator by 1. These vectors also must form invariants in the numerator, either among themselves or with the Dirac matrices of the

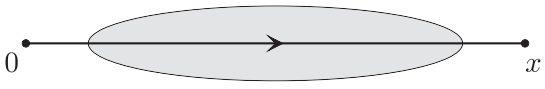

FIG. 3. A single jet with the topology of a self-energy diagram.

fermion-gluon vertices. Suppose we let z_i denote the position of the ith three-gluon vertex, and y_j the position of the jth fermion-gluon vertex. The numerator is then a product of linear combinations of invariants of the form $\not{z}_i$, $\not{y}_j$, and $z_i \cdot z_{i\prime}$. Referring to Eq. (45), one could also get factors with $z_i \cdot y_j$. Each such invariant made out of two vectors is linear in normal variables. One can see then that each fermion-gluon vertex suppresses the numerator by $\lambda^{1/2}$ at least, while every pair of three-gluon vertices produces an invariant suppressing the numerator by λ, while if a three-gluon vertex is contracted with a Dirac matrix at a fermion-gluon vertex, it also suppresses the numerator by $\lambda^{1/2}$ at least. Hence, the contribution of the numerators to γ_J is given by

$$\gamma_{n_J} \geq \frac{1}{2}(V_3^f + V_3^g) = \frac{1}{2}V_3, \tag{47}$$

with V_3^f the number of fermion-gluon vertices and V_3^g the number of three-gluon vertices inside the jet. Adding all contributions, we obtain a lower bound for the overall degree of divergence of this fermion jet,

$$\gamma_J \geq 2(V_3+V_4)+2-N_g-2N_f-V_3^g+\frac{1}{2}V_3+\mathcal{O}(\varepsilon). \tag{48}$$

Here, V_3 (V_4) is the total number of three-point (four-point) vertices, while N_g (N_f) is the number of gluon (fermion) lines in the jet. We can use the graphical identity

$$2N = E + \sum_{i=3,4} iV_i \tag{49}$$

in Eq. (48), which relates the number of lines of a diagram to the numbers of its various kinds of vertices, where E is the number of external lines of the jet. A single jet has two external lines, $E = 2$: one connected to the external point x^μ and the other to the origin. Combining the number of lines $N = N_f + N_g$ and the number of three-point vertices $V_3 = V_3^f + V_3^g$, we can rearrange the terms in Eq. (48),

$$\gamma_J \geq \frac{3}{2}V_3 + 2V_4 - N + 2 + V_3^f - N_f, \tag{50}$$

which, using the graphical identity in Eq. (49), can be reduced to

$$\gamma_J \geq 1 + V_3^f - N_f. \tag{51}$$

Here, we note that, because at each fermion-gluon vertex one fermion line enters and one exits, the number of fermion lines in the jet is equal to 1 plus the number of fermion-gluon vertices in the jet. Therefore, our power counting results in

$$\gamma_J \geq 0. \tag{52}$$

Thus, a fermion jet in coordinate space with the topology of a self-energy diagram can have at worst logarithmic divergence. In contrast to the power counting in momentum space, we did not count the number of loops, nor did we need to use the Euler identity. Note that the power counting for a scalar jet gives the same result, because the derivatives at two-scalar-gluon vertices in a scalar jet correspond to the derivatives from fermion propagators in a fermion jet. Similarly, the two-scalar-two-gluon "seagull" couplings have no numerator factors, and are counted like the four-point gluon couplings.[4]

If we had kept the terms at $\mathcal{O}(\varepsilon)$ in the power counting of Eq. (48), we would have derived a bound

$$\gamma_J \geq \left(\frac{1}{2}V_3 + V_4\right)\varepsilon, \tag{53}$$

which shows that these collinear singularities are regulated also by $\varepsilon > 0$ in coordinate space. No IR regularization is necessary after UV renormalization when the external points are taken to the light cone. However, in the Fourier transform of the vertex function for S-matrix elements in momentum space, the divergences in $p^2 = 0$ will require IR regularization with $\varepsilon < 0$ when the external points are integrated to infinity.

The power counting above and the result in Eq. (52) hold in the presence of self-energies inside the jet as well. For instance, cutting a gluon line in the jet and inserting a fermion loop does not change γ_J, because the changes due to extra fermion denominators are canceled by the terms for integrations over the positions of these two new vertices, while the denominator of the extra gluon cancels the contribution of fermion numerators to γ_J, since $\not{y}(-\not{y}) = -y^2 \sim \mathcal{O}(\lambda)$, with y^μ being the difference of the positions of the two vertices. In the case of inserting a gluon or a ghost loop, a similar cancellation occurs. The denominators of the two new lines in the loop each have a lower power by 1 compared to fermion lines, but there are now two derivatives at the new vertices raising those powers. A different power counting is needed for the case when such self-energies shrink to a point; that is $y^+ \to 0$ in the example above for a jet in the plus direction. When renormalization has been carried out, such UV divergences are removed by local counterterms.

[4]By the arguments given in the main text, the overall degree of divergence of a scalar jet is bounded from below by

$$\gamma_{SJ} \geq 2(V_3 + V_4 + V_4^{2g2s}) + 1 - N_s - N_g - V_3^g - V_3^{sg} + \frac{1}{2}(V_3^g + V_3^{sg}) + \mathcal{O}(\varepsilon),$$

with N_s the number of scalar lines, V_4^{2g2s} the number of two-scalar-two-gluon vertices, and V_3^{sg} the number of two-scalar-gluon vertices. Each term on the right-hand side cancels by Eq. (49), such that $\gamma_{SJ} \geq 0$ in this case as well.

B. Overall power counting for the vertex function

We are now ready to continue with the overall power counting for the vertex function including two jets, a soft subdiagram, and a hard subdiagram as in Fig. 2. We will do the analysis for the fermionic vertex function. As in the previous subsection, the counting is the same for the scalar vertex. It also straightforwardly extends to any amplitude for wide-angle scattering.

The homogenous soft function is independent of normal variables, and by dimensional counting it is finite for fixed external points. We introduce the notation $J^H_{(\pm)g}$ and $J^H_{(\pm)f}$ to denote the numbers of vector and fermion lines, respectively, that connect the hard subdiagram to the jets in the $\pm$ direction. In these terms, we also define

$$J^H_{g,f} = J^H_{(+)g,f} + J^H_{(-)g,f}, \tag{54}$$

$$J^H = J^H_g + J^H_f, \tag{55}$$

where J^H is the total number of lines attaching both jets to the hard subdiagram. Similarly, we define, for the lines connecting the jets to the soft subdiagram,

$$S^J_{g,f} = S^J_{(+)g,f} + S^J_{(-)g,f}, \tag{56}$$

$$S^J = S^J_g + S^J_f, \tag{57}$$

and lastly, for the lines connecting the soft and hard subdiagrams,

$$S^H = S^H_g + S^H_f. \tag{58}$$

Recall that all components of the vertices in the hard function vanish together, so that hard lines are quadratic in normal variables. Similar to Eq. (48) for a single jet, the overall degree of divergence for the vertex function relative to the lowest-order diagram can be written as

$$\begin{aligned}\gamma_\Gamma \geq\, & 4(V_3^H + V_4^H) - 2N_g^H - 3N_f^H - V_{3g}^H \\ & + \sum_{i=+,-} [2(V_3^{J_{(i)}} + V_4^{J_{(i)}}) + 2 - N_g^{J_{(i)}} - 2N_f^{J_{(i)}} - V_{3g}^{J_{(i)}} + n^{J_{(i)}}] \\ & + \mathcal{O}(\varepsilon),\end{aligned} \tag{59}$$

where $n^{J_{(\pm)}}$ denotes the numerator contributions from the jet in the $\pm$ direction. The terms labeled H are contributions from the hard part, followed by contributions from the two jets. Note that there are no contributions from integrations over the positions of soft vertices here, because all of their components are intrinsic variables.

In the hard part, every three-gluon vertex produces a vector that must be proportional to a linear combination of the position vectors z_i^μ of vertices in the hard subdiagram. These are all normal variables, and are hence order λ. These vectors may form invariants with a jet or a soft vertex suppressing the numerator by λ, or two of them may form an invariant at $\mathcal{O}(\lambda^2)$. Thus, each hard three-gluon vertex contributes $+1$ to scaling of the numerator, while their derivatives increase the power of a gluon denominator that is quadratic in λ. In total, they contribute $-V^H_{3g}$ to γ_Γ.

The numerator contributions of jets are somewhat different compared to Eq. (48), because the vectors arising from the derivatives of three-gluon vertices inside the jets can now form invariants with vectors from three-gluon vertices in the hard or soft part, or from the opposite-moving jet. At lowest order in normal variables, the invariants resulting from contracting a jet vertex with a soft vertex are zeroth order in normal variables, while those from a jet and a hard vertex are linear—which, however, we have already counted in Eq. (59) among the contributions from the hard part. There can be at most J^H_g such vectors to form out-of-jet invariants, as many as the number of lines connecting jets to the hard part. The polarization of any of the S^J_g soft gluons connecting the jets to the soft function does not produce an invariant that contributes to $n^J = n^{J^{(+)}} + n^{J^{(-)}}$, and the fermion-gluon vertices in the jets where a soft fermion line attaches do not always give a suppression in the numerator. For the minimum numerator suppressions, we can thus subtract $J^H_g + S^J_g + S^J_f$ from the total number of three-point vertices in n^J,

$$n^J \geq \frac{1}{2}(V_3^J - J_g^H - S^J), \tag{60}$$

where we use the notation of Eqs. (55) and (57).

We can again apply the graphical identity in Eq. (49) to the terms in Eq. (59) for the jets and the hard subdiagram separately. The E^H external lines of the hard function are either jet or soft lines,

$$E^H = S^H + J^H, \tag{61}$$

where we assume for this discussion that the minimum of the fermion lines connecting the jets to the hard part is two, $J^H_f \geq 2$, one from each jet. Pinch surfaces where only gluons attach the hard part to the jets in the reduced diagram are also possible and may be treated similarly, with equivalent results. These external lines must be added to the number of hard lines, $N^H = N^H_g + N^H_f$, in the identity for the total number of lines connected to the hard part,

$$2N^H + E^H = 2V_2^H + 3V_3^H + 4V_4^H. \tag{62}$$

Here, we consider the vertex of the external current as a two-point-vertex, so that $V_2^H = 1$. The total number of jet lines is related to the number of vertices in both jets by

$$2N^J + S^J = 2 + J^H + 3V_3^J + 4V_4^J, \tag{63}$$

where the number of (soft) lines, S^J, connecting the jets to the soft part is added to the number of jet lines. Removing

the contributions from the gluon lines and vertices they attach in Eq. (62), one can find a relation between the number of fermion vertices and the number of fermion lines in the hard subdiagram,

$$V_{3f}^H = N_f^H + \frac{1}{2}(S_f^H + J_f^H - 2), \tag{64}$$

while a similar relation can be found from Eq. (63) for jets,

$$V_{3f}^J = N_f^J + \frac{1}{2}(S_f^J - J_f^H - 2). \tag{65}$$

To derive a lower bound for γ_Γ in Eq. (59), it is convenient to begin by applying Eq. (62) to the H terms of γ_Γ, and Eq. (63) to the jet terms. Then, we can readily use the relations of fermion lines to vertices, Eqs. (64) and (65) for the hard subdiagram and for the jets, respectively, and the numerator inequality [Eq. (60)] to derive a lower bound for the overall degree of divergence of the vertex function:

$$\gamma_\Gamma \geq S_g^H + \frac{3}{2}S_f^H + \frac{1}{2}(S_f^J + J_f^H - 2). \tag{66}$$

The condition for a (logarithmic) divergence is then that no line can connect the hard subdiagram directly to the soft subdiagram and that only a single fermion attaches each jet to the hard subdiagram. This corresponds to similar results found for pinch surfaces in momentum space [12,15]. The soft and hard subdiagrams can only interact through jets. Moreover, when the lower bound is saturated, using the same relations above, the leftover terms in γ_Γ that are at the order of ε can be shown to be equal to

$$\gamma_\Gamma^{\mathcal{O}(\varepsilon)} = \left(\frac{1}{2}V_3^J + V_3^H + V_4^J + 2V_4^H - \frac{1}{2}[S_g^J + J_g^H]\right)\varepsilon. \tag{67}$$

For each line connecting the soft part to a jet, there is a vertex in the jet, while for each line connecting a jet to the hard part, there is a hard vertex. Thus, there will be enough vertices left over to make the coefficient of ε positive. Therefore, the logarithmic divergence of the vertex function is regulated by $\varepsilon > 0$ in coordinate space.

We shall now consider the changes in the power counting due to the removal of a vertex from one subdiagram and its inclusion in the other subdiagram. This will happen at the boundary of integration in intrinsic variables. Suppose that one of the jet vertices connected to the hard part gets captured by the hard part and becomes part of it, or a vertex in the jet escapes to the soft part, as depicted in Fig. 4. In the first case, the line, which used to connect the hard part to one of the jets, has become a hard line, while the other jet lines attached to that vertex now connect the hard part and the jet. Thus, if the vertex that gets captured is a three-gluon vertex, N_g^H, V_{3g}^H, and J^H each change by $+1$, while N_g^J and V_{3g}^J change by -1. Likewise, if a four-point vertex gets captured, N_g^H and V_4^H increase by $+1$, but J^H now increases by $+2$, while N_g^J and V_4^J change by -1. These changes, however, cancel exactly in Eq. (59) using the bound for the jet numerator contributions n^J in Eq. (60) for the most divergent configurations. Similarly, if a three-gluon vertex in the jet escapes to the soft part, it pulls two lines out of the jet, making them soft; hence N_g^J and V_{3g}^J change by -2 and -1, respectively, while S^J increases by $+1$. For a four-point vertex that escapes the jet and joins the soft part, N_g^J and V_4^J decrease by -3 and -1, respectively, while S^J increases by $+2$. These changes also cancel in Eq. (59) for the most divergent configurations. Note also that when a hard vertex escapes to the soft part, the leftover changes in Eq. (59) are equal to ΔS_H, the change in the number of lines connecting the hard and soft parts. Therefore, the leading behavior does not change, even if two different subdiagrams do overlap, as was asserted at the beginning of this section.

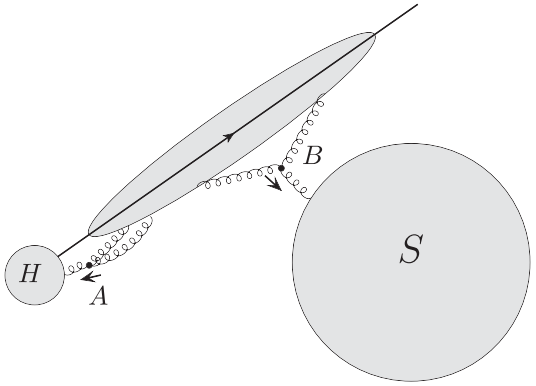

FIG. 4. A jet vertex A gets captured by the hard part, while another vertex B escapes to the soft part. Power counting for this pinch surface gives the same result as when the vertices A and B were inside the jet. The other jet in the opposite direction is suppressed here.

To conclude, we have shown by power-counting arguments that the vertex function in coordinate space can diverge at worst logarithmically times overall lowest-order behavior. This logarithmic divergence requires $D < 4$ in dimensional regularization.

V. APPROXIMATIONS AND FACTORIZATION

A fundamental consequence of the structure of pinch surfaces is the factorization of soft gluons from jets and jet gluons from the hard part. This is shown in momentum space by the use of Ward identities [14,17,21]. In this section, we show how the same Ward identities, as they appear in coordinate space, result in the factorization of soft, jet, and hard functions.

A. Hard-collinear approximation

Having identified the jet and hard regions that can give divergences in coordinate-space integrals in the previous section, we now construct a coordinate-space *hard-collinear* approximation to the integral, which enables factorization of

the jet and hard functions at the leading singularities. Recall that the only approximation made for writing a homogenous integrand to do the power counting for these two regions was dropping the terms of higher order in normal variables in lines connecting the jets to the hard part. Thus, the approximation one needs is made on the propagators of these jet lines attached to the hard part. We shall explain this hard-collinear approximation with the example of the following integral:

$$I(y) = \int d^4z J^\nu(y) g_{\nu\rho} D^{\rho\mu}(y-z) H_\mu(z), \tag{68}$$

where J^ν denotes a jet function with a direction β^ν, $D^{\rho\mu}(y-z)$ is the propagator of the line that connects a jet vertex at y to a hard vertex at z, and $H_\mu(z)$ is a hard function. We raise and lower the indices by the Minkowski metric. Here, we have suppressed the dependence on other vertices, which are also integrated over. The integral in Eq. (68) will have divergences when the jet moves in the plus or minus light-cone direction and all coordinates of the hard function vanish. In this limit, we can approximate this integral by picking out the large component of the jet, by replacing $g_{\nu\rho} \to \beta'_\nu \beta_\rho$ where $\beta^\mu = \delta^{\mu+}$ and $\beta'\nu = \delta^{\nu-}$:

$$I(y) \sim \int d^4z J^\nu(y) \beta'_\nu \beta_\rho \bar{D}^{\rho\mu}(y-z) H_\mu(z). \tag{69}$$

In the gluon propagator, $\bar{D}$, we neglect the smaller terms coming from the hard vertex. Let us take the jet to be in the plus direction; then the dependence on z^μ in the argument of the propagator will be largely through z^-, the component of the hard vertex in the opposite direction, because

$$(y-z)^2 = 2y^+(y^- - z^-) - y_\perp^2 + \mathcal{O}(\lambda^{3/2}) \tag{70}$$

for $y^+ \gg z^+$ and $y_\perp^2 \gg z_\perp^2$. We then write the propagator as

$$\begin{aligned} \beta_\rho D^{\rho\mu}(y-z) &= D^{-+}(y-z)\beta^\mu, \\ \bar{D}^{-+}(y-z) &= \frac{\partial}{\partial z^-} \int_\infty^{z^-} d\sigma D^{-+}(2y^+(y^- - \sigma\beta'^-) - y_\perp^2) \\ &\equiv \partial_{z^-} \mathcal{D}(y, z^-). \end{aligned} \tag{71}$$

For this representation, we should take $\varepsilon < 0$ in $\bar{D}^{-+}$. One can now integrate by parts in Eq. (69), so that $-\partial_{z^-}$ acts on the hard function $H_\mu(z)$:

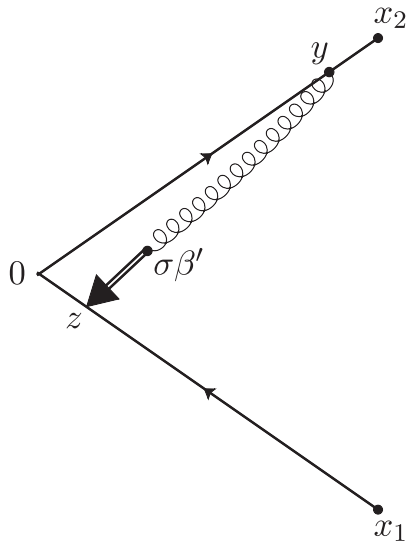

FIG. 5. One-loop example for the *hard-collinear* approximation. The arrow represents the action of the derivative on the hard function $H(z)$, which is just a fermion propagator here.

$$I(y) \sim \int d^4z J^+(y) \mathcal{D}(y, z^-)(-\partial_{z^-} H^-(z)). \tag{72}$$

There are no boundary terms as a result of integrating by parts, because in the hard function $H_\mu(z)$ there must be at least one propagator that vanishes at $z^- = \pm\infty$. Furthermore, we can add to the integrand the derivatives with respect to other components of z^μ, such that we now have a full gradient ∂_z^μ acting on the hard function $H_\mu(z)$. Because the jet function and $\mathcal{D}(y, z^-)$ do not depend on z^+ and $z_\perp$, these added terms are total derivatives and vanish after the integration. The result of our approximation can then be expressed by

$$I(y) \sim \int d^4z (J^\nu(y)\beta'_\nu) \mathcal{D}(y, z)(-\partial^\mu H_\mu(z)). \tag{73}$$

In other words, we have replaced the propagator of the gluon escaping from the jet to the hard part with $D^{\nu\mu}(y-z) \to \mathcal{D}(y,z)\beta'^\nu \partial_z^\mu$, with β'^ν being a vector in the opposite direction of the jet. The momentum-space analog of such a gluon is called "longitudinally" or "scalar polarized" and is associated with the scalar operator $\partial_\mu A^\mu(x)$ in coordinate space.

For the simplest example illustrated in Fig. 5, this approximation for the vertex function at one loop results in

$$\begin{aligned} I^{(1)} \sim \int d^D z \frac{\not{x}_2 - \not{y}}{(-(x_2-y)^2 + i\epsilon)^{2-\varepsilon}} \beta' \frac{\not{y}}{(-y^2 + i\epsilon)^{2-\varepsilon}} \int_\infty^{z^-} d\sigma \frac{1}{(-2y^+(y^- - \sigma\beta') + y_\perp^2 + i\epsilon)^{1-\varepsilon}} \\ \times \left(-\frac{\partial}{\partial z^\mu}\right) \left(\frac{-\not{z}}{(-z^2 + i\epsilon)^{2-\varepsilon}} \gamma^\mu \frac{\not{z} - \not{x}_1}{(-(z-x_1)^2 + i\epsilon)^{2-\varepsilon}} \right), \end{aligned} \tag{74}$$

where we have omitted the incoming current, integrations over jet vertices, and numerical factors. After acting with ∂_μ^z, there are two terms with a relative sign coming from the action of the derivative on either fermion propagator, canceling them in turn by the massless Dirac equation $\partial S_F(x) = -\delta^D(x)$:

$$I^{(1)} \sim \int d^D z \frac{\not{x}_2 - \not{y}}{(-(x_2-y)^2+i\epsilon)^{2-\varepsilon}} \beta' \frac{\not{y}}{(-y^2+i\epsilon)^{2-\varepsilon}} \int_\infty^{z^-} d\sigma \frac{1}{(-2y^+(y^- - \sigma\beta') + y_\perp^2 + i\epsilon)^{1-\varepsilon}} \times \left(\frac{-\not{z}}{(-z^2+i\epsilon)^{2-\varepsilon}} \delta^D(z-x_1) - \delta^D(z) \frac{\not{z} - \not{x}_1}{(-(z-x_1)^2+i\epsilon)^{2-\varepsilon}} \right). \quad (75)$$

After integrating over z, the location of the attachment of the "scalar polarized" gluon, using the delta functions, the two terms differ only in the upper limits of the σ integrals, which can be combined so that the remaining leading term is given by

$$I^{(1)} \sim -\frac{\not{x}_2 - \not{y}}{(-(x_2-y)^2+i\epsilon)^{2-\varepsilon}} \beta' \frac{\not{y}}{(-y^2+i\epsilon)^{2-\varepsilon}} \frac{-\not{x}_1}{(-x_1^2+i\epsilon)^{2-\varepsilon}} \left(\int_0^{x_1^-} d\sigma \frac{1}{(-2y^+(y^- - \sigma\beta') + y_\perp^2 + i\epsilon)^{1-\varepsilon}} \right). \quad (76)$$

Therefore, after the hard-collinear approximation, the "scalar polarized" gluon has been factored onto an eikonal line in the opposite direction from the jet of which it is a part, such that the jet is now factorized from the rest of the diagram. Note that the integration over the eikonal line is a scaleless integral, which in the limit $x_1^- \to \infty$ will be defined by its ultraviolet pole only.

The hard-collinear approximation also allows us to apply the basic Ward identities of gauge theories directly to the leading singularity of the vertex function in order to factor the "scalar polarized" gluons from the hard function. This reasoning was used in the proofs of factorization in gauge theories in momentum space [14,22–24], and the same reasoning applies here. The Ward identity that we need is given by

$$\langle \text{out}|T(\partial_{\mu_1} A^{\mu_1}(x_1) \cdots \partial_{\mu_n} A^{\mu_n}(x_n))|\text{in}\rangle = 0, \quad (77)$$

where $|\text{in}\rangle$ and $\langle \text{out}|$ are physical states involving particles of fermion and gauge fields with physical polarizations only. The gauge field $A^\mu(x)$ can be Abelian or non-Abelian; the above matrix element relation involving scalar polarized gauge fields holds at each order in perturbation theory after the sum over all contributing diagrams [25,26].

At higher orders, the external lines of the hard function will be two physical fermion lines on the light cone, one entering and the other exiting the hard function, and some number of "scalar polarized" gauge field lines with derivatives acting on the hard function. Consider the case with one such gluon line connected to the hard part as in Fig. 6. This diagram is equal to the negative of the diagram where the scalar-polarized gluon is acting on the fermion line in the opposite direction by the Ward identity [Eq. (77)], which gives a factored gluon onto an eikonal line, as we showed above at lowest order. This summarizes the argument, which was also extended to arbitrary number of gluon lines, for the proof of factorization of jets (collinear singularities) from the hard function in momentum space; see the review of Ref. [14]. The same factorization can be shown in coordinate space after the hard-collinear approximation described above using the Ward identity [Eq. (77)], in the same way as in momentum space.

B. Soft-collinear approximation

One may also do a *soft-collinear* approximation for the lines that connect the jets to the soft function, such that the collinear singularities of jets will be factored from the finite soft function. We will follow the same reasoning and repeat the same steps as we did for the hard-collinear approximation. To avoid repetition, we will skip those details of our arguments that were explained in the previous section. In analogy to the integral in Eq. (68), now consider

$$I(z) = \int d^4y S_\mu(z) D^{\mu\nu}(z-y) g_{\nu\rho} J^\rho(y). \quad (78)$$

Here, $S_\mu(z)$ denotes the soft function, and J^ρ denotes a jet function with a direction β^ρ. $D^{\mu\nu}(z-y)$ is the propagator of the line that connects a soft vertex at z to a vertex in the jet

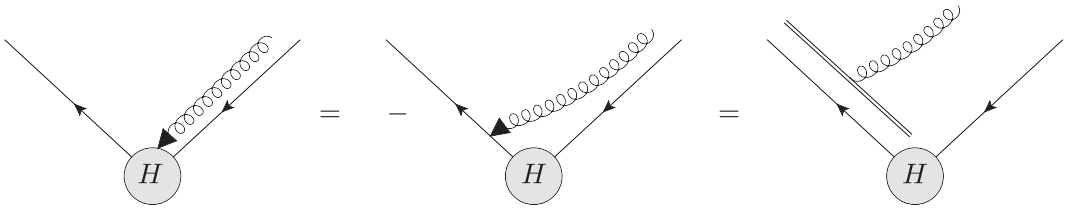

FIG. 6. Factorization of one "scalar polarized" gluon from the hard subdiagram.

at y, which are at a finite distance from each other. We suppress the dependence of either function on other vertices as before. In this integral, the only singularities of the integrand are contained in the jet function. Again, to approximate this integral, we will drop the small terms in the argument of the propagator and pick up only the large numerator component of the jet,

$$I(z) \sim \int d^4y S_\mu(z) \bar{D}^{\mu\nu}(z-y)\beta_\nu \beta'_\rho J^\rho(y), \tag{79}$$

with $\beta^2 = \beta'^2 = 0$ and $\beta \cdot \beta' = 1$. Suppose the jet is in the plus direction; then, following our power counting, $z^- \gg y^-$ and $z_\perp^2 \gg y_\perp^2$ such that

$$(z-y)^2 = 2(z^+ - y^+)z^- - z_\perp^2 + \mathcal{O}(\lambda^{1/2}). \tag{80}$$

Thus, this time we write the propagator connecting the soft part to a jet as

$$D^{\mu\nu}(y-z)\beta_\nu = \beta^\mu D^{+-}(y-z),$$
$$\bar{D}^{+-}(z-y) = \frac{\partial}{\partial y^+}\int_\infty^{y^+} d\sigma D^{+-}(z-\sigma\beta) \equiv \partial_{y^+}\mathcal{D}(z,y^+). \tag{81}$$

Using the steps above, we integrate by parts in Eq. (79), and then add to the integrand the derivatives with respect to other components of y^μ as well. In this way, we obtain

$$I(z) \sim \int d^4y S_\mu(z)\beta^\mu \mathcal{D}(y,z)(-\partial_\nu J^\nu(y)). \tag{82}$$

We see that the jets are connected to the soft part also by "scalar polarized" gluons, which can be factored from the jets by using the Ward identity given in Eq. (77). The formal proof of factorization into hard, soft, and jet functions in coordinate space now follows the momentum-space procedure and requires only the hard-collinear and soft-collinear approximations described here.

C. Eikonal approximation

Having described the hard-collinear and soft-collinear approximations above to factorize the contributions from different subdiagrams at the leading singularity, we can now think of another approximation to simplify the computation of the leading term. One may make an approximation to the integrals, keeping only the leading contribution on a pinch surface where the fermion lines are taken on the light cone, and neglecting the subleading contributions coming away from that pinch surface by imposing the results of the Landau conditions inside the integrands.

As an example, let us again take the fermionic vertex function. The solutions to Landau equations with collinear fermions set the transverse coordinates and the minus (plus) coordinates of the positions of the fermion-gluon vertices on the plus line (minus line) to zero as well as time-ordering them. These conditions can be imposed inside the integrand by replacing the fermion propagators along the plus line with

$$S_F(x^2) = \partial\Delta_F(x^2) \to \theta(x^+)\delta(x^-)\delta^2(x_\perp)\gamma\cdot\beta, \tag{83}$$

with $\beta = \delta^{\mu+}$, while for those along the minus line, in the direction $\beta' = \delta^{\mu-}$, x^+ and x^- are exchanged. This is actually the coordinate-space version of the well-known eikonal approximation, which is based on assuming the gluons are soft and neglecting their squared momenta in the fermion propagators. The eikonal approximation originates from geometrical optics, where it corresponds to the small-wavelength limit in which the trajectories of light are given by light rays as in classical theory. One might have derived the form of the fermion propagators also by taking the Fourier transform of the eikonal propagator in momentum space for a massless fermion moving in the direction $\beta^\mu = \delta^{\mu+}$,

$$\int \frac{d^4k}{(2\pi)^4}\frac{i}{\beta\cdot k + i\epsilon}e^{-ik\cdot x} = \theta(x^+)\delta(x^-)\delta^2(x_\perp). \tag{84}$$

Let us apply this eikonal approximation to the one-loop vertex diagram as an example:

$$\Gamma^{(1)}_{\text{eik}} = \int d^4y_2 d^4y_1 \theta(x_2^+ - y_2^+)\theta(y_2^+)\theta(y_1^-)\theta(x_1^- - y_1^-) \times \delta(y_2^-)\delta^2(y_{2,\perp})\delta(y_1^+)\delta^2(y_{1,\perp}) \times \frac{1}{(-(y_2-y_1)^2 + i\epsilon)}, \tag{85}$$

where we have suppressed the numerical factors and dropped the delta functions of the external lines. The result, after introducing the parameters λ and σ with $\beta'^\nu = \delta^{\nu-}$,

$$\Gamma^{(1)}_{\text{eik}} = \int_0^{x_2^+} d\lambda \int_0^{x_1^-} d\sigma \frac{1}{(-2\beta\cdot\beta'\lambda\sigma + i\epsilon)}, \tag{86}$$

is exactly equal to a first-order diagram of a Wilson line with a cusp at the origin, which begins at the point x_1^μ *pointing* in the direction of β', then changes its direction to β at the origin, and later ends at x_2^μ. The parameters λ, σ are simply relabelings for y_2^+ and y_1^- that give the locations where the gluon is attached to the Wilson line, and, of course, are integrated over. This equality between the diagrams of a cusped path-ordered exponential and of the vertex function after the eikonal approximation also holds at higher orders, because the theta functions simply order the attachments to the eikonals, while the integrations over any other vertices are the same in both cases. Therefore, we may approximate the vertex function by a Wilson-line calculation at any given order in perturbation theory [27,28]. The power counting for

the path-ordered exponentials is not exactly the same as that for the vertex function with partonic lines, but it is very similar and gives the same bound for their overall degree of divergence, which we will present in Appendix B to avoid repetition.

VI. DISCUSSION

The coordinate-space singularities of Feynman integrals in a massless gauge theory have a direct interpretation in terms of physical processes, in which classical massless particles propagate freely between points in space-time, where they scatter by local interactions. The singularities occur only if these particles move on the light cone. The condition for pinches in the coordinate integrals is interpreted as momentum conservation for these scattered particles with the identification of their momenta from their coordinates. This interpretation is the same as the interpretation given by Coleman and Norton [11] to Landau equations in momentum space [10].

The pinches in the coordinate integrals for the vertex function occur when a group of lines get mutually collinear forming jets as in momentum space. There are also pinches from "zero" lines when some set of internal vertices move to the origin $x \to 0$, reflecting a short-distance singularity, where these zero lines or vertices with vanishing components define a hard function in coordinate space. There are also end-point singularities in the integrals over Feynman parameters $\alpha \to 0$, which define the soft function in coordinate space. An important difference from the momentum space is that the soft function is finite in coordinate space when the external points of the vertex function (x_1 and x_2 above) are kept at finite distances. The collinear divergences are of ultraviolet nature in coordinate space and require $D < 4$ in dimensional regularization, while no infrared regulation is needed, since the coordinates of the external particles provide the natural infrared cutoff.

By the power-counting arguments developed above, vertex functions in coordinate space are found to be at worst logarithmically divergent at higher orders, relative to the lowest-order results. Similarly, after the eikonal approximation, the path-ordered exponentials have the same bound for their overall degree of divergence. The requirement for a divergence in both cases is that the hard and soft subdiagrams must not be directly connected, and they can only interact through the jets. Two jets on the light cone in different directions can only have a hard interaction at the origin and interact softly at later times. This illustrates in coordinate space the factorization of short- and long-distance dynamics in field theories. We have also explained the *hard-collinear* and *soft-collinear* approximations that are needed for the formal implementation of factorization in coordinate space.

The results of this study do not hold only for a specific set of massless gauge theories but are much more general. The results for vertex functions can be generalized for fixed-angle scattering at large angles, because there is no interference between incoming and outgoing jets at large angles [8,29,30]. For scattering at small angles, a different power counting for the jets is needed. Furthermore, our discussion can be extended to S-matrix elements, defining the reduction from Green functions directly in coordinate space, and eventually to cut diagrams for infrared-safe cross sections, topics which we will leave for future work.

ACKNOWLEDGMENTS

The author is grateful to George Sterman for many helpful discussions and suggestions. This work was supported by National Science Foundation Grants No. PHY-0969739 and No. PHY-1316617.

APPENDIX A: MASSIVE LINES

For completeness, we consider the extension of pinch analysis to massive lines in coordinate space. Massive lines must be explored separately because the massive propagator in coordinate space has a more complicated form; it can be written in $4-2\varepsilon$ dimensions by

$$\Delta_F(x;m) = \left(\frac{-i}{8\pi^2}\right)\int_0^\infty d\xi \left(\frac{2\pi i}{\xi}\right)^\varepsilon \times \exp\left[i\left(-\frac{x^2}{2}\xi - \frac{m^2}{2\xi} + i\epsilon\right)\right]. \quad \text{(A1)}$$

Since the massive propagator does not have a simple denominator, we cannot do a Feynman parametrization. However, using Eq. (1), we can combine the propagators of each line of an arbitrary Feynman diagram with massive lines:

$$\tilde{I}(\{x_i^\mu\}) = \prod_{\text{lines } j}\int_0^\infty d\xi_j \prod_{\text{vertices } k}\int d^D y_k \exp[-i\tilde{D}(\xi_j, x_i, y_k)] \times \tilde{F}(\xi_j, x_i, y_k), \quad \text{(A2)}$$

where ξ_j is now the parameter of the jth line with dimensions of mass squared. The phase $\tilde{D}$ of the exponent is given directly from Eq. (A1) by

$$\tilde{D}(\xi_j, x_i, y_k) = \sum_j \xi_j \frac{z_j^2}{2} + \frac{m_j^2}{2\xi_j}, \quad \text{(A3)}$$

with z_j^μ a linear function of the external coordinates $\{x_i^\mu\}$ and the positions of (internal) vertices $\{y_k^\mu\}$ as before. The functions $\tilde{F}(\xi_j, x_i, y_k)$ include constants and the "numerators," which might come from derivatives of three-point vertices acting on the exponentials.

One can obtain the Landau conditions from the integral representation in Eq. (A2) for diagrams with massive lines by the method of stationary phase. The conditions of

stationary phase with respect to the positions of internal vertices,

$$\frac{\partial}{\partial y_k^\mu}\tilde{D}(\xi_j, x_i, y_k) = \sum_{\text{lines } j \text{ at vertex } k} \eta_{jk}\xi_j z_j^\mu = 0, \quad \text{(A4)}$$

where $\eta_{jk} = +1(-1)$ if the line j ends (begins) at vertex k and is zero otherwise, give exactly the same result as Eq. (9) for the massless case because the masses of the lines do not depend on the positions of the internal vertices. The phase is stationary with respect to the ξ parameters when

$$\frac{\partial}{\partial \xi_r}\tilde{D}(\xi_j, x_i, y_k) = z_r^2 - \frac{m_r^2}{\xi_r^2} = 0. \quad \text{(A5)}$$

For massive lines, the stationary points are given by

$$\xi_r = \frac{m_r}{\sqrt{z_r^2}}, \qquad z_r^2 > 0. \quad \text{(A6)}$$

If the mass of the line r is zero, Eq. (A5) is only satisfied if its coordinates have a lightlike separation, irrespective of the value of ξ_r.

Repeating the same reasoning as in the massless case, we identify the product $\xi_r z_r^\mu$ with a momentum vector p_r^μ for line r, while this time ξ_r is determined by Eq. (A6). The time component of this momentum vector,

$$p_r^0 = m_r \frac{z_r^0}{\sqrt{(z_r^0)^2 - |\vec{z}_r|^2}} = \frac{m_r}{\sqrt{1-\beta_r^2}}, \quad \text{(A7)}$$

equals the energy of a classical particle with mass m_r propagating with the speed of $\beta_r = |\vec{z}_r|/z_r^0$. Therefore, we can interpret the stationary phases in the integral representation [Eq. (A2)] in the same way as pinch singularities explained in Sec. II—as a physical process in space-time where classical particles propagate between vertices with their momenta conserved at each vertex.

APPENDIX B: POWER COUNTING FOR PATH-ORDERED EXPONENTIALS

We shall lastly do the power counting for the vacuum expectation value of path-ordered exponentials with constant lightlike velocities meeting at a cusp. Consider one Wilson line, which starts from the point $x_1^\mu = x_1\delta^{\mu-}$ in the $\beta_1^\mu = \delta^{\mu-}$ direction and meets the other line at the origin; the other line moves in the $\beta_2^\mu = \delta^{\mu+}$ direction and ends at the point $x_2^\mu = x_2\delta^{\mu+}$. Formally, we consider the diagrams for the vacuum expectation value of the following operator:

$$\Gamma_{\beta_1,\beta_2}(x_1, x_2) = \langle 0|T(\Phi_{\beta_2}(x_2, 0)\Phi_{\beta_1}(0, x_1))|0\rangle \quad \text{(B1)}$$

with constant-velocity-ordered exponentials,

$$\Phi_{\beta_i}(x+\lambda\beta_i, x) = \mathcal{P}\exp\left(-ig\int_0^\lambda d\lambda' \beta_i \cdot A(x+\lambda'\beta_i)\right). \quad \text{(B2)}$$

As for the vertex function, there may be divergences when some vector and/or fermion lines get collinear to the eikonal lines forming two jets, which can interact softly at large distances and have a hard interaction at the cusp.

In analogy to Eq. (59) for the vertex function, the overall degree of divergence of such path-ordered exponentials in coordinate space can be written with a bound from below,

$$\begin{aligned}\gamma^{\text{eik}} \geq\ & w^H + 4(V_3^H + V_4^H) - 2N_g^H - 3N_f^H - V_{3g}^H \\ & + \sum_{i=+,-}[2(V_3^{J_{(i)}} + V_4^{J_{(i)}}) - N_g^{J_{(i)}} - 2N_f^{J_{(i)}} - V_{3g}^{J_{(i)}} \\ & + \frac{1}{2}(V_3^{J_{(i)}} - S_{(i)}^J - J_{(i)g}^H + w^{J_{(i)}})],\end{aligned} \quad \text{(B3)}$$

with w^H being the total number of hard lines attached to the Wilson lines and $w^{J_{(\pm)}}$ the number of attachments of the jet in the $\pm$ direction to the Wilson line in the same direction. The lines that connect a jet to the Wilson line in the opposite direction are soft lines and are counted together with the connections of the jet to the soft subdiagram by $S_{(i)}^J$.

In Eq. (B3), we have added a term $+w^H$ for the integrations over the locations of the attachments of the hard subdiagram to the eikonals to the contributions from the hard part, because these connections have to move to the cusp so that all components of these hard lines vanish. Furthermore, the derivatives at each three-gluon vertex will bring vectors that form invariants in the numerator, which will be of the form of either $(\beta_i \cdot z)$ or $(z \cdot z')$. The number of vectors β_i that can show up in the numerator is equal to the sum of the number of attachments to each Wilson line. The net effect from all three-gluon vertices in the hard subdiagram is given by the term $-V_{3g}^H$, as for the vertex function. In a jet, a three-gluon vertex z that is connected to the Wilson line in the same direction as the jet produces an invariant $(\beta_i \cdot z)$ linear in λ in the numerator, while one connected to the opposite Wilson line produces an invariant zeroth order in λ. Therefore, we add $w^J = w^{J_{(+)}} + w^{J_{(-)}}$ to the number of jet three-point vertices for the term for the minimum numerator suppressions in γ^{eik} and subtract the connections of the jets to the opposite eikonals with those to the soft subdiagram.

The relations of the number of lines to the number of the vertices for the jets and the hard subdiagram are in this case slightly different from Eqs. (62) and (63) for the vertex function:

$$2N^H + J^H + S^H = w^H + 3V_3^H + 4V_4^H, \quad \text{(B4)}$$

$$2N^J + S^J = w^J + J^H + 3V_3^J + 4V_4^J, \quad \text{(B5)}$$

for the hard part and the jets, respectively. Similarly, the relation between the number of fermion lines and the fermion-gluon vertices in the hard part is given by

$$V_{3f}^{H} = N_f^H + \frac{1}{2}(S_f^H + J_f^H), \tag{B6}$$

while for the jets they are related by

$$V_{3f}^{J} = N_f^J + \frac{1}{2}(S_f^J - J_f^H). \tag{B7}$$

Note also that $J_f^H \geq 0$ in this case. Plugging these graphical identities for the subdiagrams into Eq. (B3), we find

$$\gamma^{\text{eik}} \geq S_g^H + \frac{3}{2}S_f^H + \frac{1}{2}(S_f^J + J_f^H). \tag{B8}$$

Any direct connection between the hard and soft subdiagrams and fermion lines connecting any two subdiagrams suppresses the integral as for the vertex function. The collinear singularities of path-ordered exponentials with constant lightlike velocities are also at worst logarithmic in coordinate space [31].

[1] R. J. Eden, P. V. Landshoff, D. I. Olive, and J. C. Polkinghorne, *The Analytic S-Matrix* (Cambridge University Press, Cambridge, England, 1966).
[2] L. J. Dixon, L. Magnea, and G. F. Sterman, J. High Energy Phys. 08 (2008) 022.
[3] Z. Bern, L. J. Dixon, D. C. Dunbar, and D. A. Kosower, Nucl. Phys. **B425**, 217 (1994).
[4] R. Britto, F. Cachazo, B. Feng, and E. Witten, Phys. Rev. Lett. **94**, 181602 (2005).
[5] L. J. Dixon, J. Phys. A **44**, 454001 (2011).
[6] R. Britto, J. Phys. A **44**, 454006 (2011).
[7] G. P. Korchemsky and G. Marchesini, Nucl. Phys. **B406**, 225 (1993).
[8] S. M. Aybat, L. J. Dixon, and G. F. Sterman, Phys. Rev. D **74**, 074004 (2006).
[9] J. M. Drummond, G. P. Korchemsky, and E. Sokatchev, Nucl. Phys. **B795**, 385 (2008); J. M. Drummond, J. Henn, G. P. Korchemsky, and E. Sokatchev, Nucl. Phys. **B795**, 52 (2008).
[10] L. D. Landau, Nucl. Phys. **13**, 181 (1959).
[11] S. Coleman and R. E. Norton, Nuovo Cimento **38**, 438 (1965).
[12] G. Sterman, Phys. Rev. D **17**, 2773 (1978).
[13] G. Date, Ph.D. thesis, SUNY, Stony Brook, 1982 (Report No. UMI-83-07385).
[14] J. C. Collins, D. E. Soper, and G. Sterman, Adv. Ser. Dir. High Energy Phys. **5**, 1 (1988).
[15] G. F. Sterman, in *Boulder 1995, QCD and beyond* (World Scientific, Singapore, 1996), pp. 327–406.
[16] R. C. Hwa and V. L. Teplitz, *Homology and Feynman Integrals* (W. A. Benjamin, Inc., New York, 1966).
[17] G. Sterman, *An Introduction to Quantum Field Theory* (Cambridge University Press, Cambridge, England, 1993).
[18] J. Hadamard, Acta Math. **22**, 55 (1899).
[19] F. Cachazo, arXiv:0803.1988.
[20] J. S. Ball and T.-W. Chiu, Phys. Rev. D **22**, 2542 (1980).
[21] J. Collins, *Foundations of Perturbative QCD* (Cambridge University Press, Cambridge, England, 2011).
[22] G. T. Bodwin, Phys. Rev. D **31**, 2616 (1985); **34**, 3932(E) (1986).
[23] J. C. Collins, D. E. Soper, and G. Sterman, Nucl. Phys. **B261**, 104 (1985).
[24] J. C. Collins, D. E. Soper, and G. Sterman, Nucl. Phys. **B308**, 833 (1988).
[25] G. 't Hooft, Nucl. Phys. **B33**, 173 (1971).
[26] G. 't Hooft and M. J. G. Veltman, Nucl. Phys. **B50**, 318 (1972).
[27] G. P. Korchemsky and A. V. Radyushkin, Nucl. Phys. **B283**, 342 (1987).
[28] O. Erdogan and G. Sterman, arXiv:1112.4564.
[29] G. Sterman and M. E. Tejeda-Yeomans, Phys. Lett. B **552**, 48 (2003).
[30] S. Catani, Phys. Lett. B **427**, 161 (1998).
[31] I. A. Korchemskaya and G. P. Korchemsky, Phys. Lett. B **287**, 169 (1992).